Instrument Science Report WFC3 2008-23

WFC3 TV3 Testing: UVIS-1′ Dark Frames and Rates

A.R. Martel
August 19, 2008

ABSTRACT

WFC3 underwent its third thermal vacuum testing in the Space Environment Simulation Chamber at the Goddard Space Flight Center over a two-month period in the winter and spring of 2008. Throughout this campaign, dark frames were acquired for the UVIS-1′ flight detector at several operating temperatures. In this report, we present an analysis of these dark frames. At the nominal on-orbit parameters of -82 C, gain of 1.5 e^-/DN and four-amplifier readout, we measure a dark current rate of ~0.23 e^-/hour/pix for the AB chip and a slightly higher value of ~0.29 e^-/hour/pix for the CD chip. In the long integration dark frames (3000 sec) at -82 C, a "glow" is seen along the lower edge of the C and D quadrants (but along the top edge of the A and B quadrants for binnings of 2x2 and 3x3). At the warmer temperatures (> -49 C), a narrow (width of ~115 pix), horizontal, curved track becomes visible from the center of the left edge of quadrant C out to a spot in quadrant D. The CD chip has a greater fraction of hot pixels than the AB chip, by a factor of 1.2-1.5. The temperature dependence of the dark current rates is consistent with the dark current equation from ~-82 C to ~22 C. The dark current rate meets the CEI specification for temperatures colder than -50 C.

Introduction

Dark frames were obtained for the flight detector UVIS-1′ (CCD18 – amplifiers C and D, CCD178 – amplifiers A and B) of WFC3 as part of the Thermal Vacuum 3 (TV3) campaign at the Goddard Space Flight Center (GSFC) in the winter and spring of 2008.

These darks will serve as a comparison baseline for monitoring the on-orbit behavior of the dark current and the growth of hot pixels. They also represent the first set of dark frames to be used in the creation of the reference files for processing the early datasets from the Servicing Mission Orbital Verification by the WFC3 pipeline. Previous analyses of the WFC3/UVIS dark frames have been presented for previous incarnations of the UVIS detector in Baggett & Hilbert (2004; ambient/UVIS-1), Hilbert & Baggett (2004; ambient/UVIS-1), Hilbert & Baggett (2005; TV1/UVIS-1), Hilbert (2007; ambient/UVIS-2), and Martel (2007; TV2/UVIS-2). In this report, we present the analysis of the dark frames for the instrument in its final configuration and with its flight UVIS detector. The format of this report follows closely that of ISR 2007-26 (TV2/UVIS-2).

The Data

In Table A1 in Appendix A, we list the dark frames included in this study. Although the nominal period of TV3 was 2008/02/20 to 2008/04/21 (IDs 48658 to 59262), the sample was supplemented with the 20 sec dark frame 48477 in order to provide an additional warm dark rate (16.5 C). Only the frames at the cold temperatures of -81.9 C (binnings of 1x1, 2x2, and 3x3) were acquired as part of dedicated SMSs (UV01S03A and UV01S04A), the remainder coming from the imaging portion of the System Functional Test or from the 10-image Servicing Mission 4 Functional Test at the warm temperature of the detector at the time of execution. The temperature of -81.9 C is close to the planned orbital setpoint of -83 C and so the results presented here should be comparable to those obtained in orbit. Only full frames with the standard four-amplifier readout (ABCD) and gain of 1.5 e^-/DN are considered.

Because the dark current rate is so low at the coldest temperature of -81.9 C, we find that the combination of several frames of long integration times is necessary to reach sufficient S/N ratios for accurate measurements. Moreover, this combined dark frame must be corrected with a ‘superbias’ of the same temperature; a single bias frame would introduce too much noise. Multiple frames also permit the efficient removal of the contaminating cosmic ray hits, thus providing a more reliable estimate of the population of hot pixels. Hence, single dark frames with matching single bias frames at -82 C, such as those in the UVIS Science Monitor (SMS UV28S01H), are not included in this report. Frames acquired in special modes, such as charge injection and post-flash, are excluded, as well as frames that show the signature of hysteresis, in particular the "bowtie" anomaly (Bushouse & Lupie 2005) and PSF spots from the alignment verification.

Analysis

Image Processing

All dark frames were processed with a Python class specifically written to process ground-based WFC3 images (Martel 2008). For each image, a linear fit through the serial virtual overscan region was first subtracted from each quadrant. The four quadrants were then assembled into one image and the overscan regions were trimmed. For a given temperature, an average dark frame was then created with the PyRAF 'imcombine' task and the 'crrej' option to eliminate any cosmic-ray hits. Bias frames acquired at the same temperature, amplifier readout, binning, and commanded gain as the dark frames, and as close as possible in time (usually within the same SMS), were processed in a similar way and subtracted from the average dark frames. The resultant frame was then converted to rate units of e^-/hour.

Dark Rate Calculation

We modeled the dark current rate as the mode of the histogram of the rate in each quadrant using a Gaussian fit to the peak while excluding the hot pixel tail. Our Python method offers the option of fitting the Gaussian above a certain fraction of the peak to avoid the contribution of the hot pixels. At cold operating temperatures (-81.9 C), this level is very low, about 0.01% of the peak or less. At warmer temperatures, the hot pixel tail becomes significant and so the user can specify only a portion of the right wing of the main peak to include in the fit. We note that this approach is very similar to that used by the ACS team to calculate the on-orbit dark rate of the Wide Field Channel (M. Sirianni, private communication). The counts in each bin of the Gaussian are used as weights in calculating the final error on the rates.

Results

The Dark Frames

The dark images are shown in Fig. 1 for operating temperatures of -81.9 C, -49.1 C, and 19.5 C after subtraction of matching bias frames. The warmest dark shows a periodic, diagonal striation pattern in the general orientation of the Amp B to Amp C axis. Similar bands were also seen in the warm darks of the UVIS-2 detector (Martel 2007). The width of the bands is approximately 250 pixels (10″). Both warm frames show a horizontal "track" from the center of the left edge of the amp C quadrant, where it is brightest, to a diffuse spot in the Amp D quadrant. The track sharply curves down ~300 pixels (12″)

from the left edge and remains roughly horizontal at a distance of ~400 pixels (16″) from the bottom of the frame. It ends at the spot in quadrant D. The width of the track is about 115 pixels (4.6″) and the diameter of the spot is 160 pixels (6.4″). The counts at the center of the spot are a factor of four above the surrounding background. A faint "glow" is also seen in the upper-left corner of quadrant C. It does not extend into the neighboring quadrant A. These three features are not new; they were observed in ambient testing at GSFC in 2004 (see Fig. 1 of Hilbert & Baggett 2004). But the track and spot were not present in the UVIS-2 detector and the glow was at a different location (Martel 2007).

At a temperature of -81.9 C (top panel), the dark frame is relatively clean except for an enhancement near the center of its bottom edge. This "glow" spans both quadrants C and D but appears slightly offset towards quadrant D. A vertical slice through the frame shows that the counts rise slowly, starting ~800 pixels from the bottom, up to 4.5 times the level at the center of the frame. Curiously, a similar glow is also present in the 2x2 and 3x3 binned dark frames but at the top edge of the AB chip, with a slight offset in quadrant A (Fig. 2).

The nature of the glows is unknown. Their origin is unlikely external – the SES lamps were off during the execution of the dark SMSs (UV01S03A and UV01S04A), and even so, the features do not have the signature shape, location, and intensity of stray light leaking into the instrument, as seen in the light leak test of Jan 3, 2008, when WFC3 was in SSDIF. We also confirm that the glows are present in each dark frame that was co-added into the final average dark for each binning. Hence the glows are not the result of a sporadic effect in one (or a few) of the darks. There is also no active, "warm" CCD component near the vicinity of the glows. Potentially, these features could result from a non-complete flush before the dark exposures. But according to the logs, there was no strong illumination of the detector, such as a flat field, before the darks, only a series of bias frames (as part of SMSs UV01S03A and UV01S04A). Glow-like features in the central part of the chip may also indicate CTE-related issues, which would be more likely to appear in the central portion of the chip (A. Waczynski, private communication). But the fact that the location of the glow is inverted top-to-bottom between the non-binned and binned frames may suggest that it is the result of the readout timing pattern itself. The diagonal bands may be due to the laser annealing used in the manufacturing process and the track and spot in the bottom chip may similarly be the result of the manufacture.

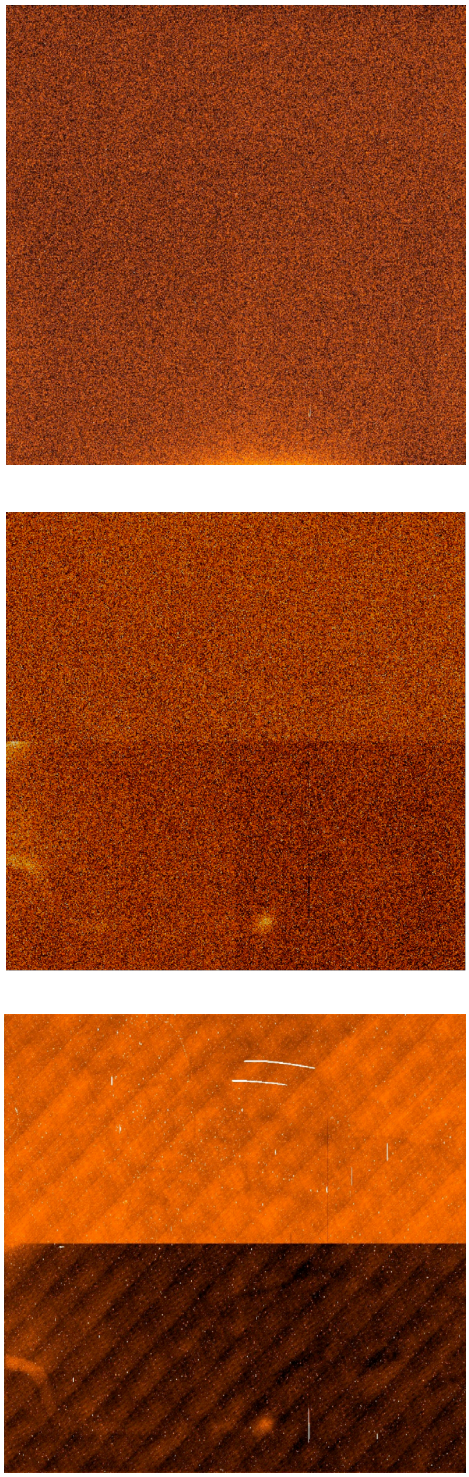

Figure 1: WFC3 UVIS-1′ dark frames after full-frame bias subtraction at -81.9 C (top), -49.1 C (middle) and 19.5 C (bottom) at gain=1.5 e^-/DN in standard orientation (amp A in top-left corner and amp D in bottom-right corner) and 1x1 binning. All overscan regions have been trimmed.

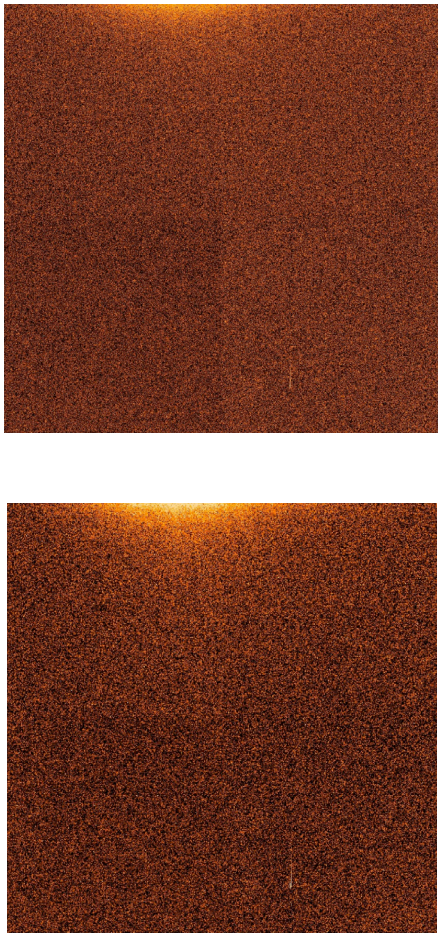

Figure 2: WFC3 UVIS-1′ dark frames after full-frame bias subtraction at -81.9 C and gain=1.5 e^-/DN in standard orientation and binnings of 2x2 (top) and 3x3 (bottom).

The Dark Current Rate

The dark current rates for temperatures of -81.9 C are tabulated in Table 2 for binnings of 1x1, 2x2, and 3x3. The conversion from counts to electrons was made using the gains tabulated in Baggett (2008). As an example of our analysis, the dark rate histograms for binning 1x1 for each amplifier are shown in Fig. 3. The mean rates for all four amplifiers are : 0.26 e^-/hour/pix (1x1), 1.58 e^-/hour/pix (2x2), and 2.98 e^-/hour/pix (3x3). These values are well below the Contract-End-Item specification 4.6.4 of < 20 e^-/hour/pix.

Table 1. Dark Current Rate in e^-/hour/pix

Amplifier	**-81.9 C 1x1**	**-81.9 C 2x2**	**-81.9 C 3x3**
A	0.216 ± 0.001	1.98 ± 0.01	3.84 ± 0.01
B	0.250 ± 0.001	1.94 ± 0.01	3.37 ± 0.01
C	0.277 ± 0.001	0.97 ± 0.01	2.48 ± 0.01
D	0.302 ± 0.001	1.43 ± 0.01	2.24 ± 0.01

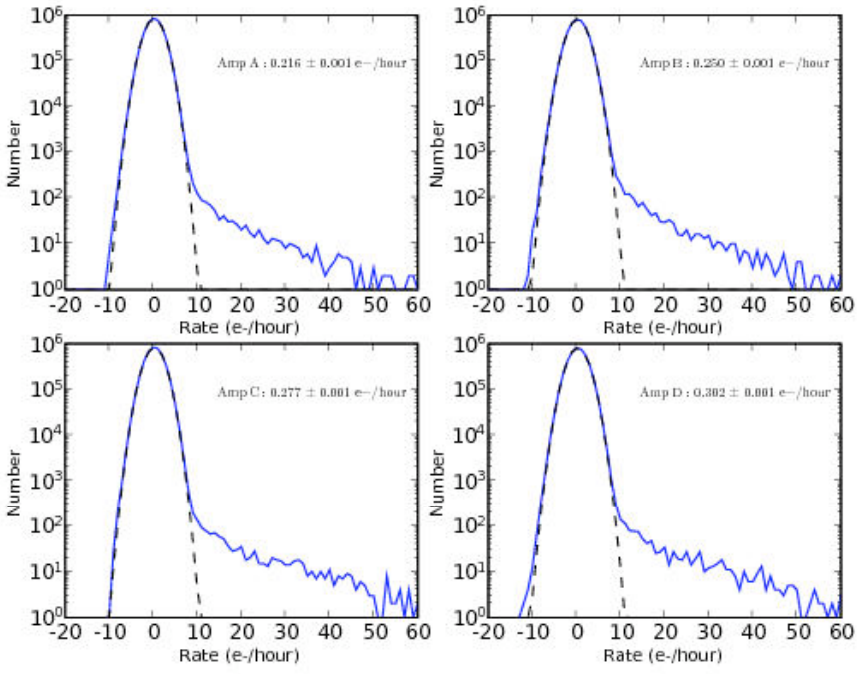

Figure 3: Histograms of the dark current rate in each quadrant of the average dark frame at a temperature of -81.9 C (gain=1.5). The dashed line is the Gaussian fit to the peak.

The Hot Pixels

The population of hot pixels can be analyzed when the average dark frame can be assembled from three or more dark frames, insuring a robust removal of cosmic ray hits which particularly affect the longest exposures (3000 sec). For the nominal detector temperature of -81.9 C, we define hot pixels as those with a count rate of ≥20 e^-/hour/pix, well away from the main Gaussian peak (see Fig. 3). This value is chosen arbitrarily and should be increased for warmer temperatures.

In Table 2, the fraction of hot pixels in each quadrant and their mean count rates are listed. The CD chip has more hot pixels than the AB chip, by a factor of about 1.2-1.5. The mean hot pixel rates are similar in all quadrants but lowest in quadrant C and highest in quadrant B. The spatial distribution of the hot pixels over the whole frame appears random.

Table 2. Hot Pixel Fraction and Mean Count Rate (-81.9 C, gain=1.5)

Amplifier	**Fraction (%)**	**Mean Rate (e^-/hour/pix)**
A	0.0069	65
B	0.0089	85
C	0.0106	60
D	0.0105	75

The Temperature Dependence

Throughout the TV3 campaign, several dark frames (and their associated bias frames) were acquired at "warm" temperatures at the nominal gain of 1.5 e^-/DN and four-amplifier readout (ABCD). These are listed in Table A1. We can therefore perform a rough analysis of the behavior of the dark rate with temperature. In Fig. 4, we plot the distributions of the dark rates for four of these warm temperatures. As expected, the growth of the hot pixel tail and the increase in the dark current rate, as indicated by the shift of the main peak towards higher counts, are extremely sensitive to the temperature. The periodic bumps in the dark rate distributions at the warmest temperatures are likely due to the broad striations in those dark frames (see bottom of Fig. 1, for example).

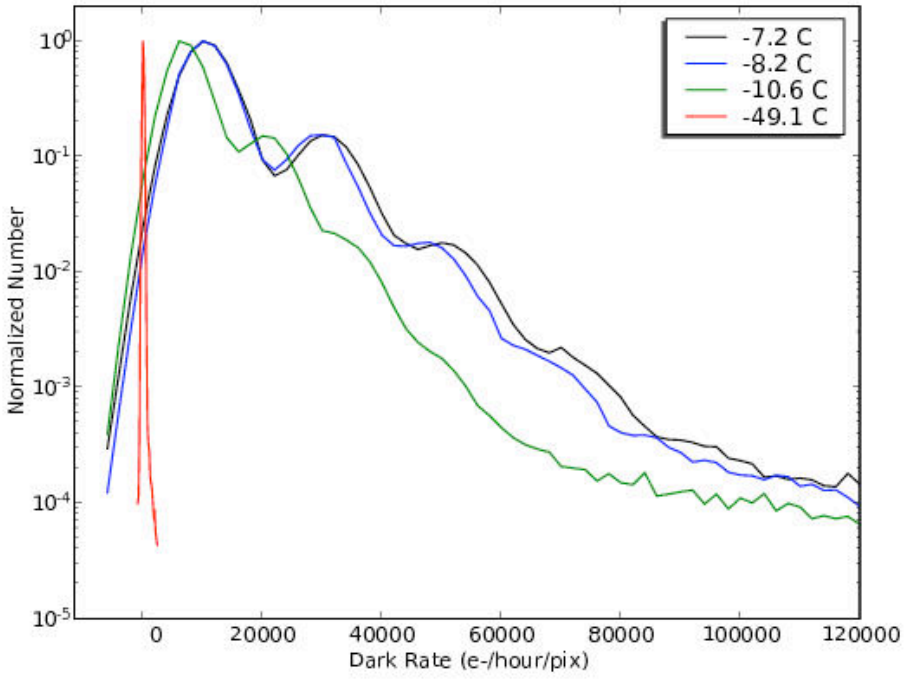

Figure 4: Distributions of the dark count rates at warm temperatures normalized to their peak values (amp D only).

The dark rates measured at the warm temperatures are listed in Table 3 for each amplifier. Comparing the dark rates between the two chips, we see that the AB chip has a consistently higher rate than the CD chip, typically by a factor of ~1.6-2.0. But for the coldest temperature of -81.9 C, this relation is opposite : the CD chip has a slightly higher rate than the AB chip (see Table 1). This disparity is likely due to the slight increase in counts coming from the glow along the lower edge of the CD chip in the cold dark, as discussed above. No edge glows are observed in any of the warm darks listed in Table 3.

With these additional temperatures, we find that the CEI specification is met for temperatures colder than about -50 C. Although we have made no distinction in the dark rates between the two MEBs, mostly because of the dearth of dark frames taken on each electronic side, the -8.2 C data hint that the MEB1 rates are ~4% greater than the MEB2 rates for all four amplifiers.

Table 3. Dark Current Rate at Warm Temperatures in e^-/hour/pix (gain=1.5, 1x1)

Temperature (Celsius)	**MEB**	**A**	**B**	**C**	**D**
-49.2	1	26.81 ± 0.08	24.72 ± 0.08	27.01 ± 0.07	16.43 ± 0.08
-49.1	2	22.35 ± 0.08	24.46 ± 0.08	19.38 ± 0.08	7.75 ± 0.08
-10.6	2	15030 ± 2	15391 ± 2	7813 ± 2	7222 ± 2
-8.2	1	21975 ± 3	22355 ± 3	11702 ± 2	10714 ± 2
-8.2	2	21056 ± 3	21384 ± 3	11264 ± 2	10382 ± 2
-7.2	1	22936 ± 3	23181 ± 3	11789 ± 2	10830 ± 2
16.5	1	518845 ± 30	518145 ± 30	312265 ± 20	301720 ± 20
19.5	1	813030 ± 40	810860 ± 40	513690 ± 25	496100 ± 25
21.5	2	1061500 ± 55	1057585 ± 55	678255 ± 30	655885 ± 30

We can verify that our measurements behave as predicted by the dark current equation (Janesick 2001). This expression is D_R (e^-/hour/pix) = $3600 \cdot C \cdot T^{1.5} \cdot \exp(-E_g/2kT)$ where C is a constant, T is the operating temperature in Kelvins, E_g is the silicon bandgap energy in eV given by $E_g = 1.1557 - 7.021 \times 10^{-4} \cdot T^2/(1108+T)$, and *k* is Boltzmann's constant (8.62×10^{-5} eV/K). The equation only needs to be solved for the scaling factor C. The fits are shown in Fig. 4 for the two chips; the measurements agree generally well with the model except for all amplifiers at -50 C, which show an unusually low dark current rate.

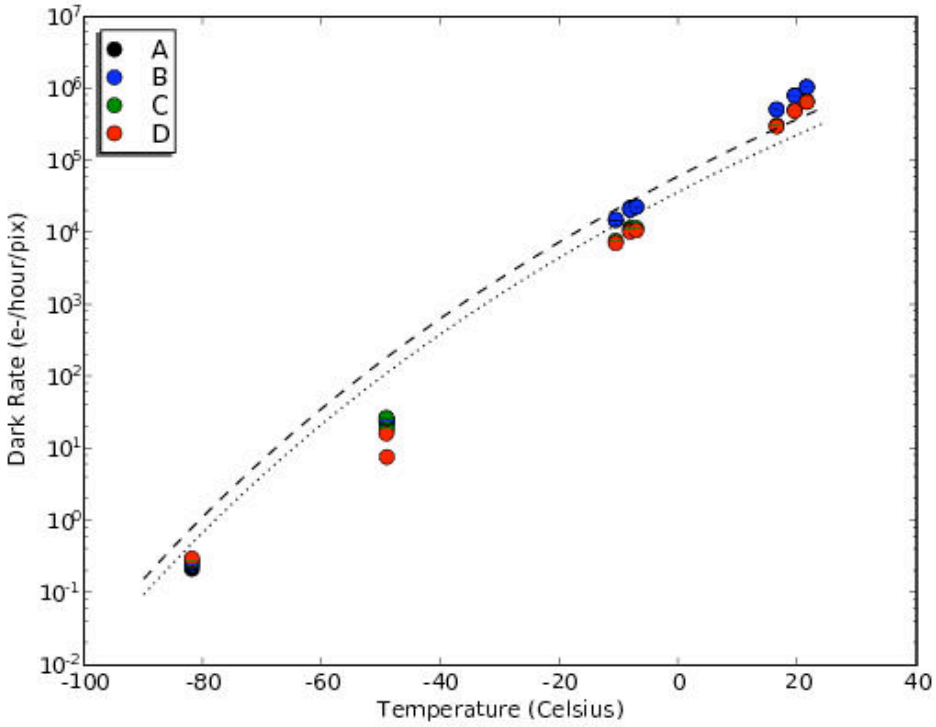

Figure 4: The dark rate measurements (gain=1.5) for the UVIS-1′ detector are modeled with the dark current equation (dashed line: amps AB, dotted line: amps CD).

Conclusions

We have assembled a set of dark frames at different operating temperatures for the WFC3 UVIS-1′ detector. These were acquired in the final thermal vacuum campaign of the instrument at GSFC. At the nominal configuration of four-amplifier readout, gain of 1.5 e^-/DN, and a binning of 1x1, the overall dark rate is ~0.26 e^-/hour/pix. The dark current rate meets the Contract-End-Item specification 4.6.4 of < 20 e^-/hour/pix for temperatures colder than about -50 C and behaves as predicted by the dark current equation from -82 C to 22 C.

References

Baggett, S. & Hilbert, B. 2004, WFC3 ISR 2004-01, "Readnoise and Dark Current in WFC3 Flight CCD Ambient Data"

Baggett, S. 2008, WFC3 ISR 2008-13, "2008-13: WFC3 TV3 Testing: UVIS-1' Gain Results"

Bushouse, H., & Lupie, O. 2005, WFC3 ISR 2005-20, "WFC3 Thermal Vacuum Testing: UVIS Science Performance Monitor"

Hilbert, B. 2007, WFC3 ISR 2007-10, "WFC3 Ambient Testing: UVIS Dark Current Rate"

Hilbert, B., & Baggett, S. 2004, WFC3 ISR 2004-13, "WFC3 UVIS Dark Current and Readnoise from Ambient Testing"

Hilbert, B., & Baggett, S. 2005, WFC3 ISR 2005-13, "Results of WFC3 Thermal Vacuum Testing - UVIS Readnoise and Dark Current"

Janesick, J.R. 2001, Scientific Charge-Coupled Devices, SPIE Press, p. 622

Martel, A.R. 2007, WFC3 ISR 2007-26, "WFC3 TV2 Testing: UVIS-2 Dark Frames and Rates"

Martel, A.R. 2008, WFC3 ISR 2008-02, "Python Quick-Look Utilities for Ground WFC3 Images"

Appendix A.

The OPUS-processed UVIS-1′ dark frames analyzed in this report are ordered by their temperature in Table A1. All the frames were taken in the standard four-amp readout mode (ABCD) and with a commanded gain of 1.5 e^-/DN. The database ID number of the dark frames, their associated bias frames, their integration time, and their binning are listed in columns 1 to 4, respectively. The operating temperature of the detector (column 5) is taken from the IUVDETMP header keyword. The frames were acquired with either MEB1 or MEB2 (column 6). The observation date is tabulated in the last column.

Table A1. Dark Frames in WFC3 Thermal Vacuum 3 Campaign

Dark ID	Bias ID	Integration Time (sec)	Binning	Temperature (Celsius)	MEB	Observation Date
50845 50847 50849 52288 52290 52292	50843, 50844 50846, 50848 50850 52286, 52287 52289, 52291 52293	3000	1x1	-81.9	1	2008/03/11
48703, 48704	48702	100	1x1	-49.2	1	2008/02/22
48679, 48680	48678	100	1x1	-49.1	2	2008/02/21
49204	49203	20	1x1	-10.6	2	2008/03/05
52785	52784	20	1x1	-8.2	1	2008/03/21
52795	52794	20	1x1	-8.2	2	2008/03/21
49186	49185	20	1x1	-7.2	1	2008/03/04
48477	48476	20	1x1	16.5	1	2008/02/09
48659	48658	20	1x1	19.5	1	2008/02/20
48669	48668	20	1x1	21.5	2	2008/02/21
56895 56903	56887-56894 56896-56902	1000	2x2	-81.9	2	2008/04/08
56919 56937	56904-56918 56920-56936	1000	3x3	-81.9	2	2008/04/08